Supplemental Material : Interactive Exploration of Vivid Material Iridescence based on Bragg Mirrors

[1]G. Fourneau, [1]R. Pacanowski, [1]P. Barla
[1]INRIA

In this supplemental document, we discuss our choice of using a piecewise-constant instead of a piecewise-linear spectral approximation for RGB rendering (Section 1), we provide further evaluation results of this approximation (Section 2) and of our single-reflection spectral BRDF model (Section 3). Finally, we provide technical instructions to run the provided BRDF Explorer application (Section 4).

1 Piecewise-constant vs piecewise-linear approximations

In the paper, we use a piecewise-constant approximation for the reflectance spectrum of a Bragg mirror. Although a piecewise-linear approach might seem more accurate or efficient, it is not the case as we show in the following.

For both approximations, we use the same spectral landmarks and we sample the same spectral reflectance envelope, then use the correction factor from Appendix B in the paper. As shown in Figure 1 (using the same parameters as Figure 3 in the paper), the piecewise-linear approximation consistently overestimates reflectance, in particular close to band gap edges where the envelope is steeply increasing or decreasing. In contrast, the piecewise-constant approximation overestimates parts of the reflectance, but underestimates others, yielding a better result.

The error is worse when the slope of the enveloppe is even steeper, which happens when a band gap narrows as shown in Figure 2. The issue persists even when subdividing the approximation into 8 pieces between consecutive band gaps. One could partially reduce this effect by making subdivisions proportional to the slope magnitude, but implementing such a solution would be more costly and less straightforward compared to our current solution.

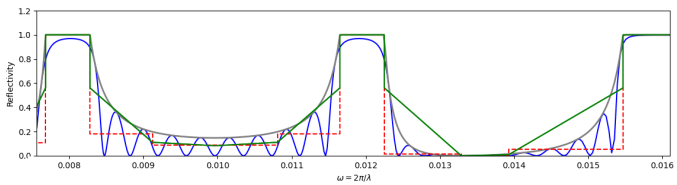

FIGURE 1 – We compare the piecewise-linear (in green) and piecewise-constant (in dashed red) approximations, both using the correction factor (see Appendix B in the paper), used to account for loss of energy due to oscillations. The piecewise-linear approximation tends to over-estimate the reference (in blue) near band gap edges.

Similarly to a piecewise-constant approximation, a piecewise-linear approximation may be efficiently integrated against CMFs via Look-Up Tables (LUTs). While in the former case, we only need one LUT, in the latter we need two, which we write $L(\lambda)$ and $C(\lambda)$. Indeed, if we consider a given linear piece $R_L(\lambda, a, b) = a\lambda + b$ for $\lambda \in [\lambda_0, \lambda_1]$, its integrated value over a CMF $f(\lambda)$ becomes :

$$I = \int_{\lambda_0}^{\lambda_1} R_L(\lambda, a, b) f(\lambda) d\lambda = F(\lambda_1, a, b) - F(\lambda_0, a, b),$$

with $F(\bar{\lambda}, a, b)$ given by :

$$\begin{aligned} F(\bar{\lambda}, a, b) &= \int_0^{\bar{\lambda}} (a\lambda + b) f(\lambda) d\lambda, \\ &= a \int_0^{\bar{\lambda}} \lambda f(\lambda) d\lambda + b \int_0^{\bar{\lambda}} f(\lambda) d\lambda, \\ &= aL(\bar{\lambda}) + bC(\bar{\lambda}). \end{aligned}$$

Nevertheless, adopting this solution would necessitate twice as many LUT fetches compared to our piecewise constant implementation. Figure 3 compares the linear and constant methods. The constant approximation employs twice as many pieces (i.e., is subdivided one additional time) as the linear approach, resulting in an equal number of LUT fetches for both methods. The piecewise-approximation yields consistently better results.

Given that a piecewise-linear approximation is more resource-intensive, more complex to implement, and raises issues near band gaps, we chose the piecewise-constant approximation for our approach.

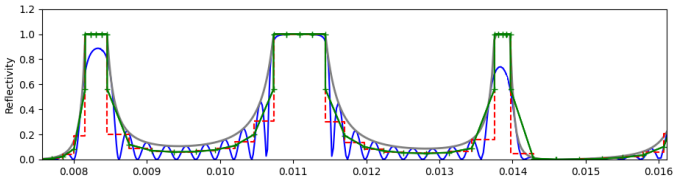

FIGURE 2 – Even with more subdivisions, the piecewise-linear approximation behaves poorly near thin band gaps.

2 Spectral approximation for RGB

All timings are measured on PC with a Quadro P5000 NVIDIA Card and all images are generated using the BRDFExplorer binaries provided as supplemental materials.

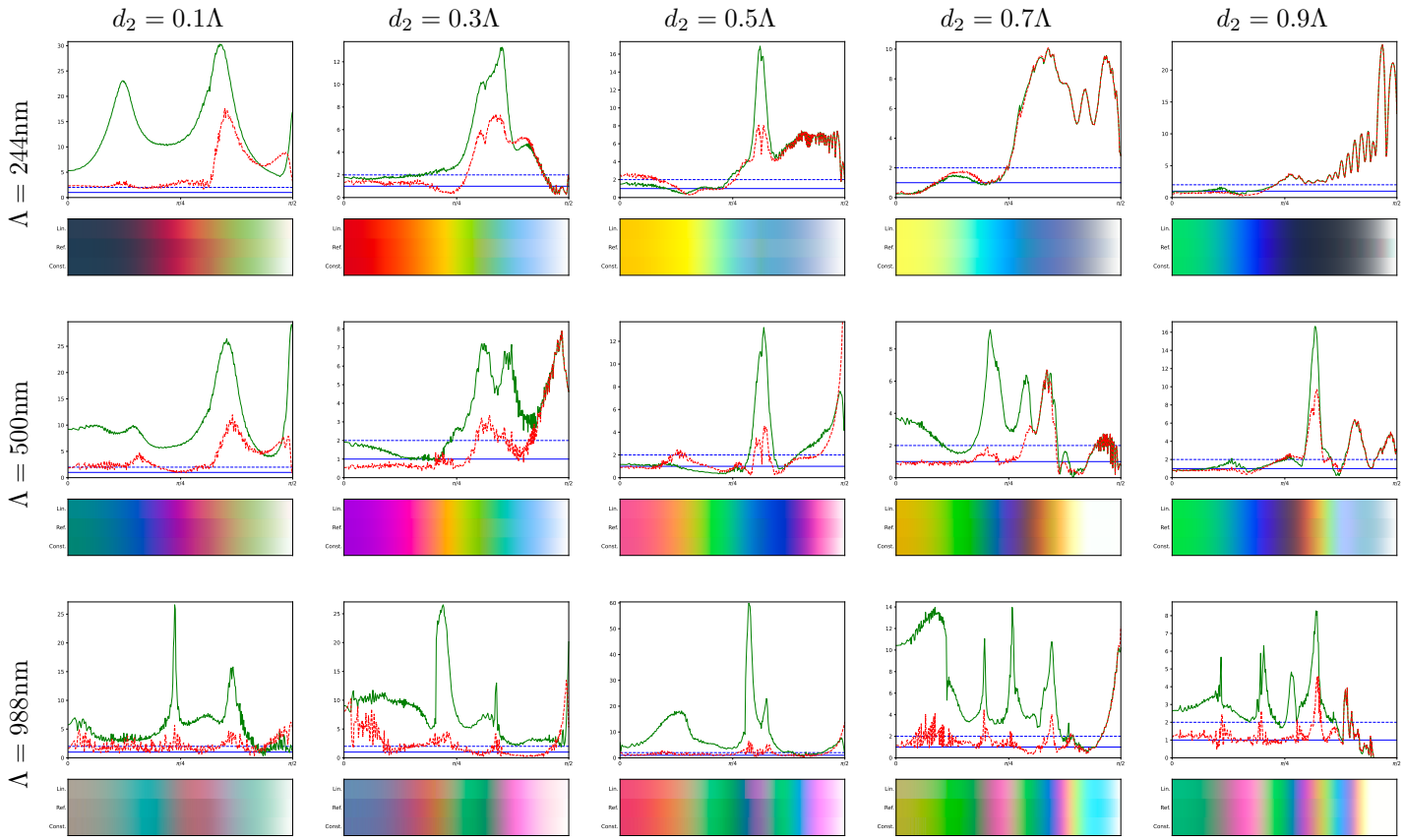

FIGURE 3 – Plots of color differences (ΔE CIE2000) between the reference spectra (see Figure 3 in the paper) and the piecewise-linear approximation subdivided once (in green), or the piecewise-constant approximation subdivised twice (in dashed red). Both approximations require an equal number of LUT fetches. The piecewise-constant approximation performs consistently better, particularly at high Λ values. The blue horizontal lines indicate thresholds for color differences : $\Delta E = 1$ (solid lines) for differences imperceptible to the human eye, and $\Delta E = 2$ (dashed lines) for differences perceptible through close observation. Below each plot we show color gradients obtained from the reference (center) and the different approximations (piecewise-linear on top, piecewise-constant at bottom).

The supplemental video shows a live demonstration of our RGB model, where Bragg parameters are manipulated interactively and their effect on appearance is commented.

Figures 4, 5 and 6 present rendered images using our different approximations, for three values of Λ respectively. The other material parameters remain fixed : $n_1 = 1$, $n_2 = 1.5$, $d_1 = d_2 = 0.5\Lambda$ and $\alpha = 0.05$. Each image is compared against the reference solution (first column). All renderings are done at 512spp and a $1K$ resolution. Difference images decrease in magnitude with increasing values of s, as summarized by SMAPE metrics. We observe that for $\Lambda = 244$nm and $\Lambda = 500$nm, there is little improvement for $s > 3$, while for $\Lambda = 988$nm we already obtain a satisfying SMAPE for $s = 3$. For that reason, we pick $s = 3$ as a good trade-off when using the subdivided approximation. Figure 7 shows a smooth Bragg mirror with spatially-varying parameters, which renders in real-time.

3 Single-reflection BRDF model

In Figure 8, we validate our optimized BRDF simulation (using pre-integrated transmission) against the naive simulation. The two versions are visually indistinguishable. Note that the last configuration yields identical results by design, since all light paths transmitted by the rough Bragg layer are absorbed. We compare our optimized simulation to the naive simulation in Table 1 in terms of efficiency, which is computed based on rendering times and the SMAPE metric as described in the main paper. Our optimized simulation yields similar average SMAPE than a naive simulation in a smaller time, yielding better efficiency.

	time (sec)	Avg. SMAPE	Eff.
Naive sim.	55−160−158	0.013−0.044−0.02	1076−351−794
Optim. sim.	35−82−84	0.018−0.041−0.034	1268−737−879

TABLE 1 – Comparison of optimized vs naive BRDF simulations on the three configurations of Table 2 in the paper, using $7.5K$spp at 40×40 resolution. We use ground truth renderings at $120k$ spp and the same resolution to compute SMAPE. They take 814, 2511 and 2511 seconds.

In order to validate our single-reflection BRDF model, we compare it against a simulation restricted to light paths that undergo a single reflection in the layered Bragg structure (SR sim.). As shown in Figure **??**, the differences are once again negligible. Comparisons in terms of efficiency can be found in the paper.

In Figure 10, we show renderings obtained with our single-reflection BRDF model for all the Bragg mirror configurations of Figure 4 in the main paper, using a single Bragg layer of roughness $\alpha = 0.1$ on top of a diffuse base with $\rho_d = 0.1$. As a matter of comparison, we also show in Figure 11 renderings for similar Bragg layers, this time under a smooth coating, again using our single-reflection BRDF model. The only difference is that $n_1 = 1.4$ and $n_2 = 1.6$.

In Figure 12 we show the diffuse base component corresponding to renderings of Figure 9 (top) in the paper. Since light paths go through the rough Bragg layer before reaching the diffuse base, the diffuse component of the BRDF is itself colored in a way that depends on Bragg parameters.

The supplemental video shows a live demonstration of our single-reflection spectral model on an Intel Xeon W-2135 3.70 GHz equipped with a Nvidia GeFOrce RTX 280 GPU. The lookup tables corresponding to Yeh reflectance and integrated transmittance must be recomputed any time a Bragg parameter is modified. Thanks to the transmission filter, this takes place interactively, in less than 40ms. The transmission filter must be recomputed anytime roughness is modified, which takes around 600ms. Note that transmission filters for several roughness values could be precomputed in order to further improve edition performance, but we have not found this to be necessary.

4 BRDF Explorer

We provide an implementation of our RGB model as a BRDF Explorer shader (`braggOptim.brdf`). We also provide BRDF Explorer binaries (64 bit) for Windows, Linux and MacOS (Intel CPU only). To reproduce the results of the supplemental video, one needs to select BRDF importance sampling as the rendering strategy in the Lit Object view of BRDF Explorer and adjust the number of samples and passes as desired.

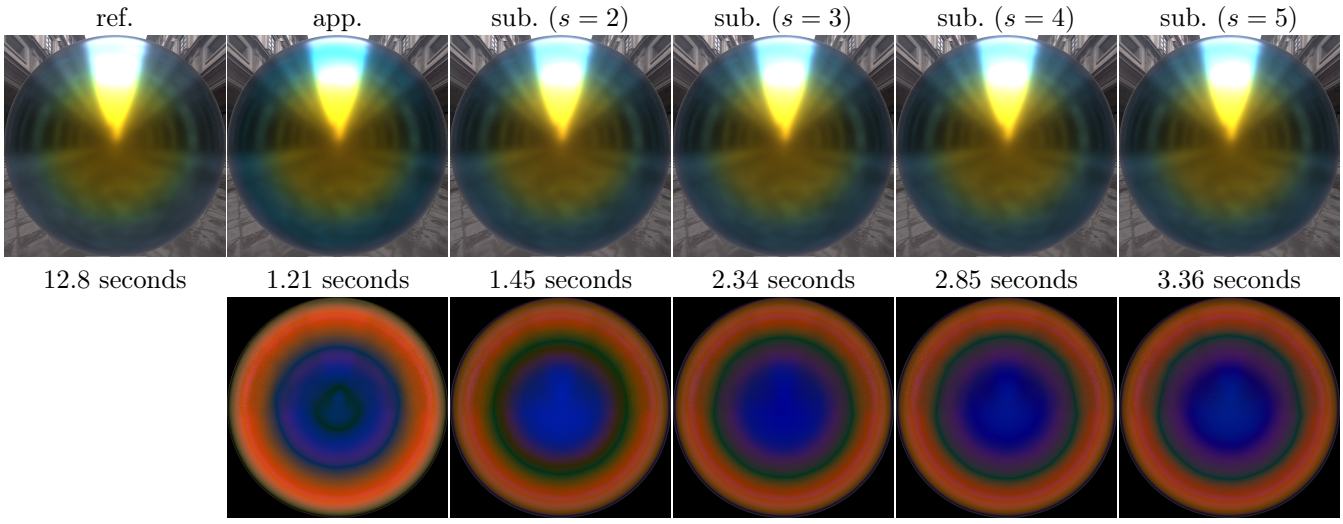

FIGURE 4 – **RGB rendering comparisons (using $\Lambda = 244$nm)** between the reference (left column) and different approximations : without (app.) and with subdivisions (sub.) using different values for s. The second row shows the difference images against the reference, computed using the SMAPE metric.

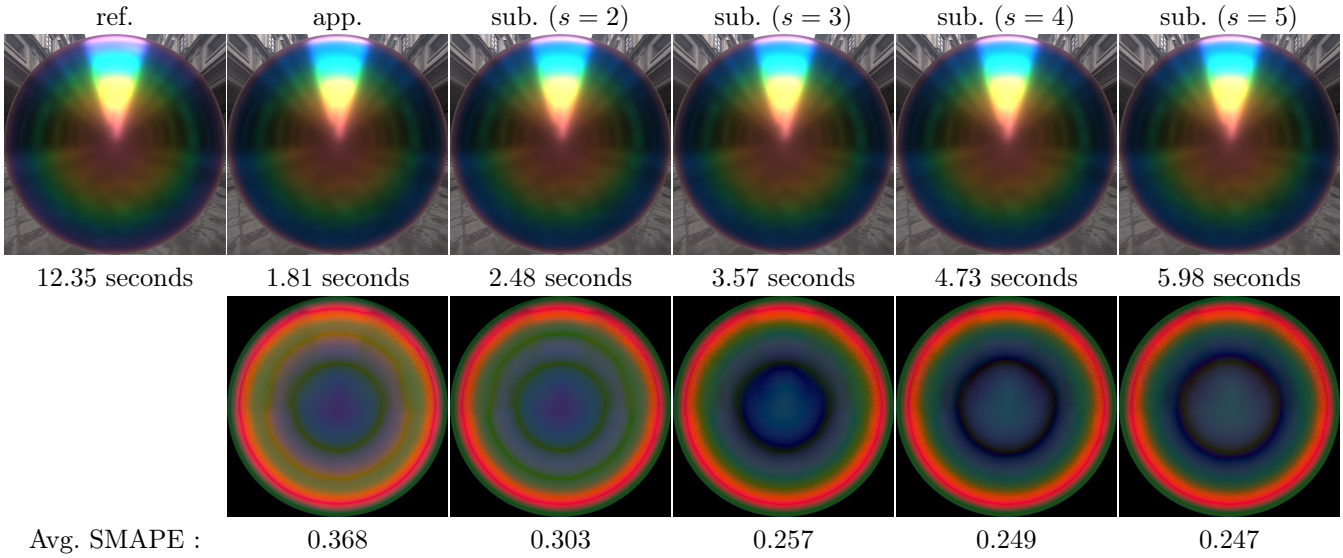

FIGURE 5 – **RGB rendering comparisons (using $\Lambda = 500$nm)** between the reference (left column) and different approximations : without (app.) and with subdivisions (sub.) using different values for s. The second row shows the difference images against the reference, computed using the SMAPE metric.

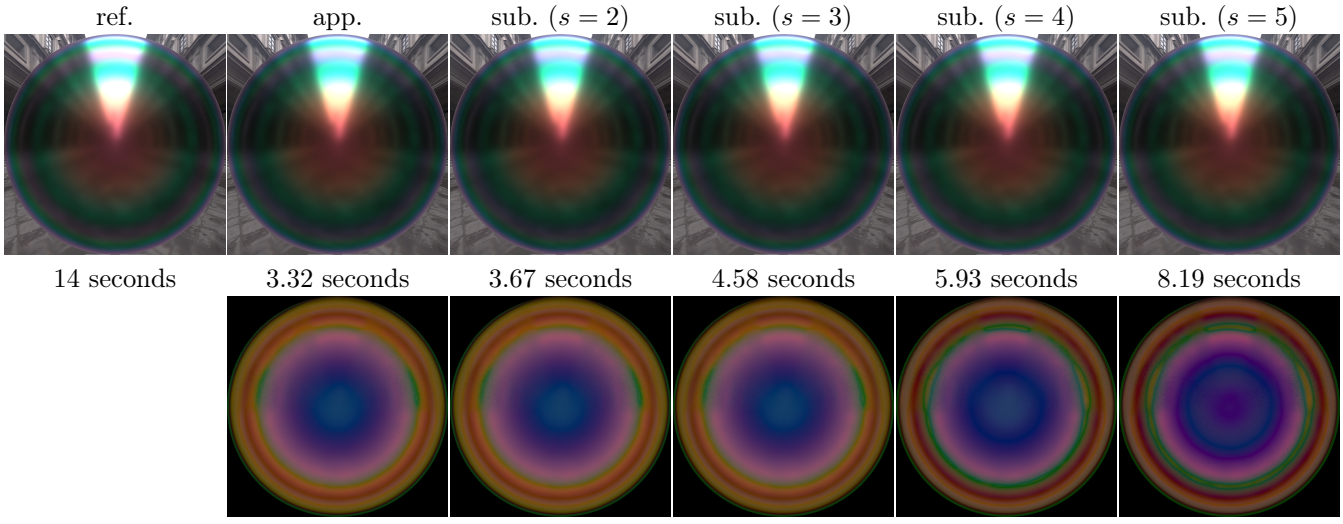

FIGURE 6 – **RGB rendering comparisons (using $\Lambda = 988$nm)** between the reference (left column) and different approximations : without (app.) and with subdivisions (sub.) using different values for s. The second row shows the difference images against the reference, computed using the SMAPE metric.

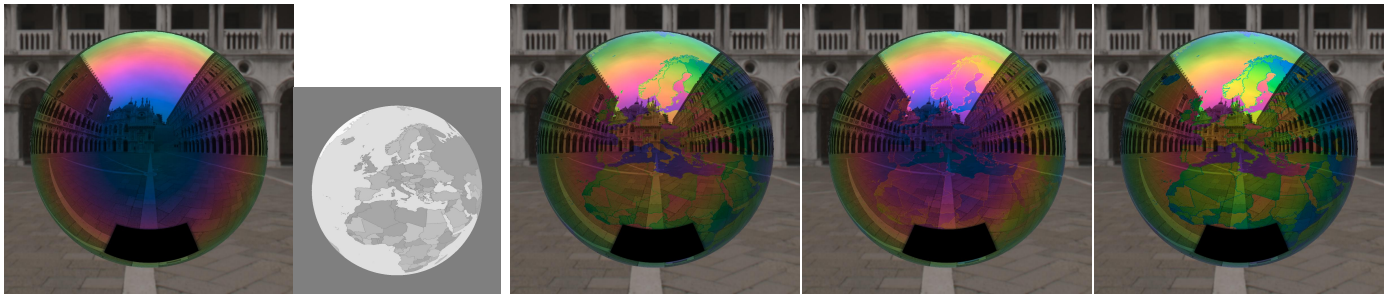

(a) Static Λ & δ (b) texture $T(\mathbf{x})$ (c) Using $\Lambda(\mathbf{x})$ (d) Using $\delta(\mathbf{x})$ (d) Using $\Lambda(\mathbf{x})$ & $\delta(\mathbf{x})$

FIGURE 7 – **Spatial variations of Bragg parameters.** We start with (a) a sphere made of a homogeneous smooth Bragg mirror ($n_1 = 1$, $n2 = 1.5$, $\Lambda = 500$nm, $\delta = d_1/\Lambda = 0.15$), rendered with our RGB model in the Doge environment map. Using the texture map $T(\mathbf{x})$ in (b), we let vary the Λ and δ parameters separately in (c) and (d), and conjointly in (e), using the following pair of functions : $\Lambda(\mathbf{x}) = \Lambda(0.5 + 0.5T(\mathbf{x}))$ and $\delta(\mathbf{x}) = \delta^{T(\mathbf{x})}$.

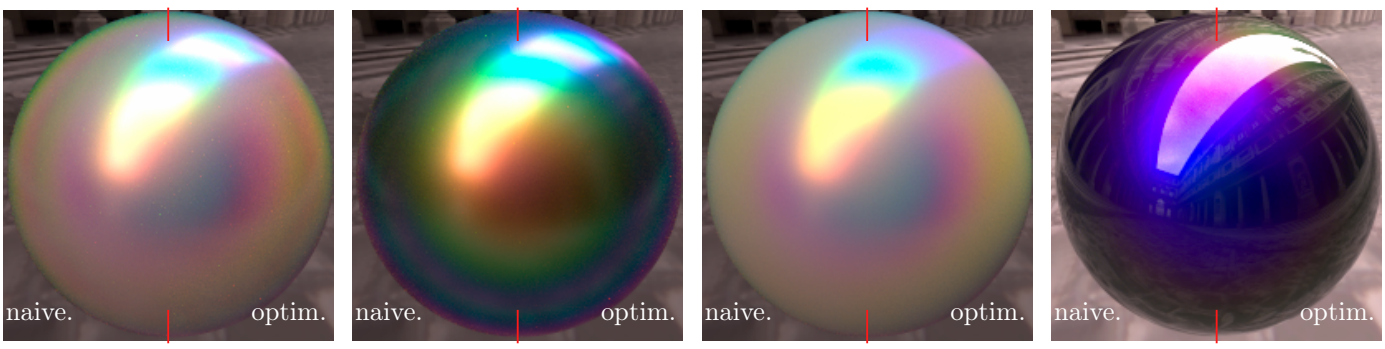

FIGURE 8 – **Validation of our optimized simulation** against a ground-truth simulation on four layered Bragg structures (columns).

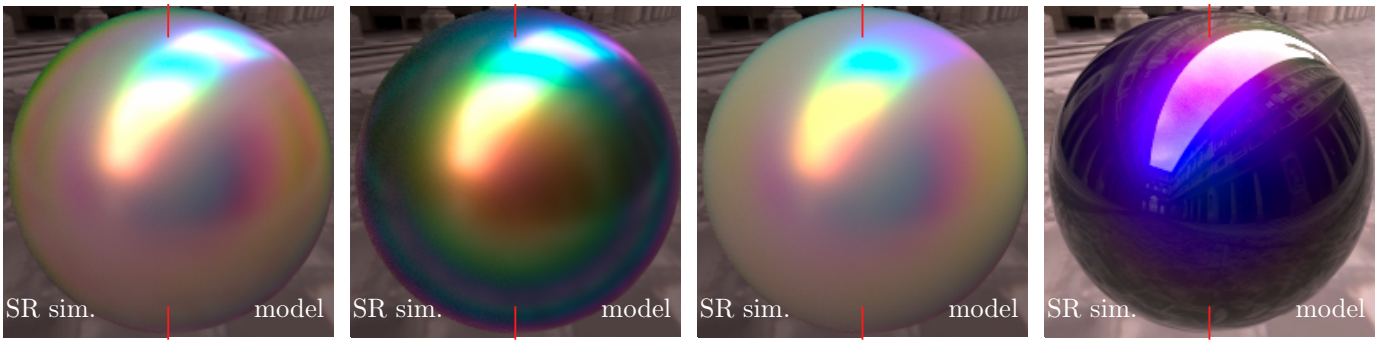

FIGURE 9 – **Validation of our single-reflection model** against a reference single-reflection simulation, on four layered Bragg structures (columns).

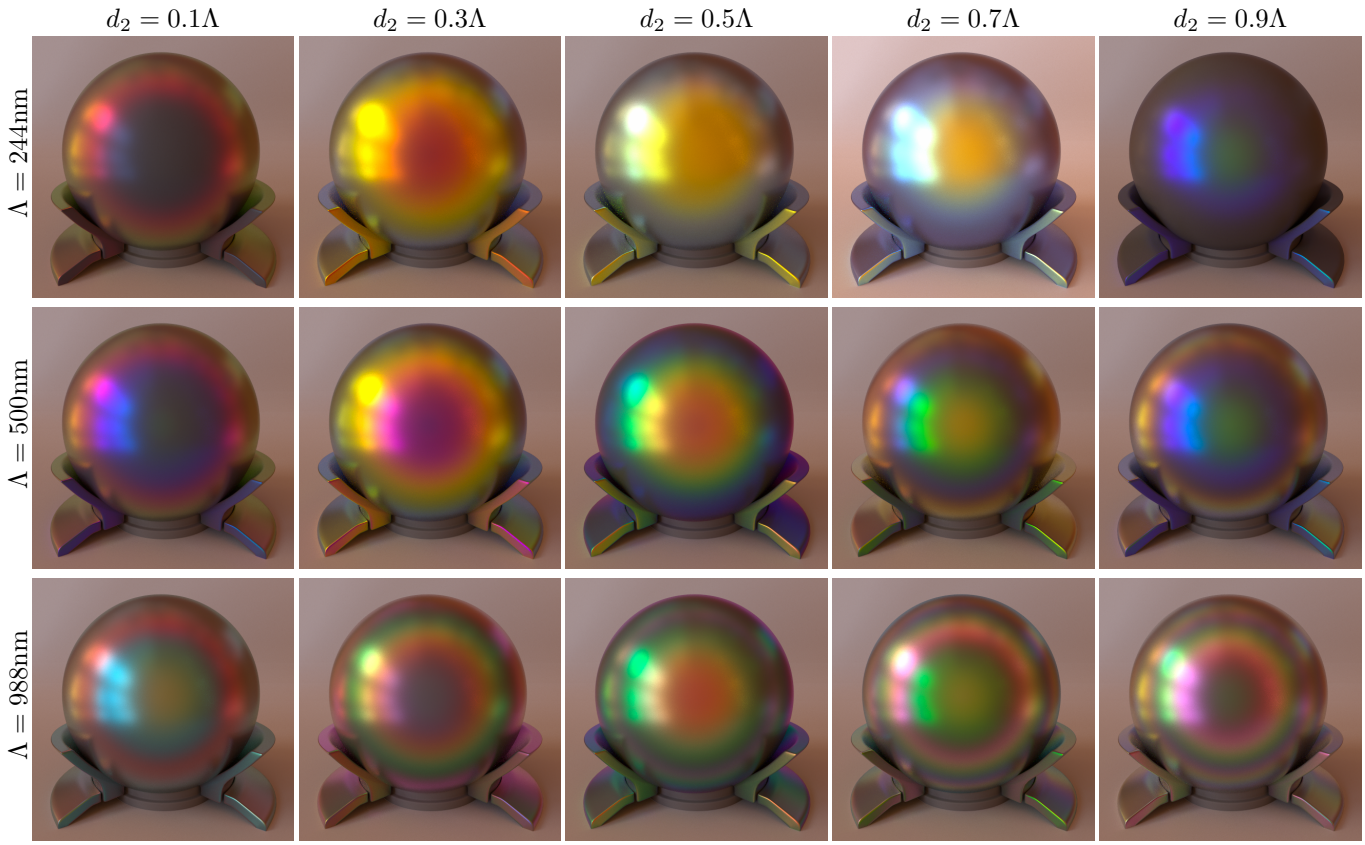

FIGURE 10 – **Exploration of rough Bragg appearance**, using Bragg parameters from Figure 4 in the paper on a Bragg layer of roughness $\alpha = 0.1$, on top of a diffuse base of albedo $\rho_d = 0.1$.

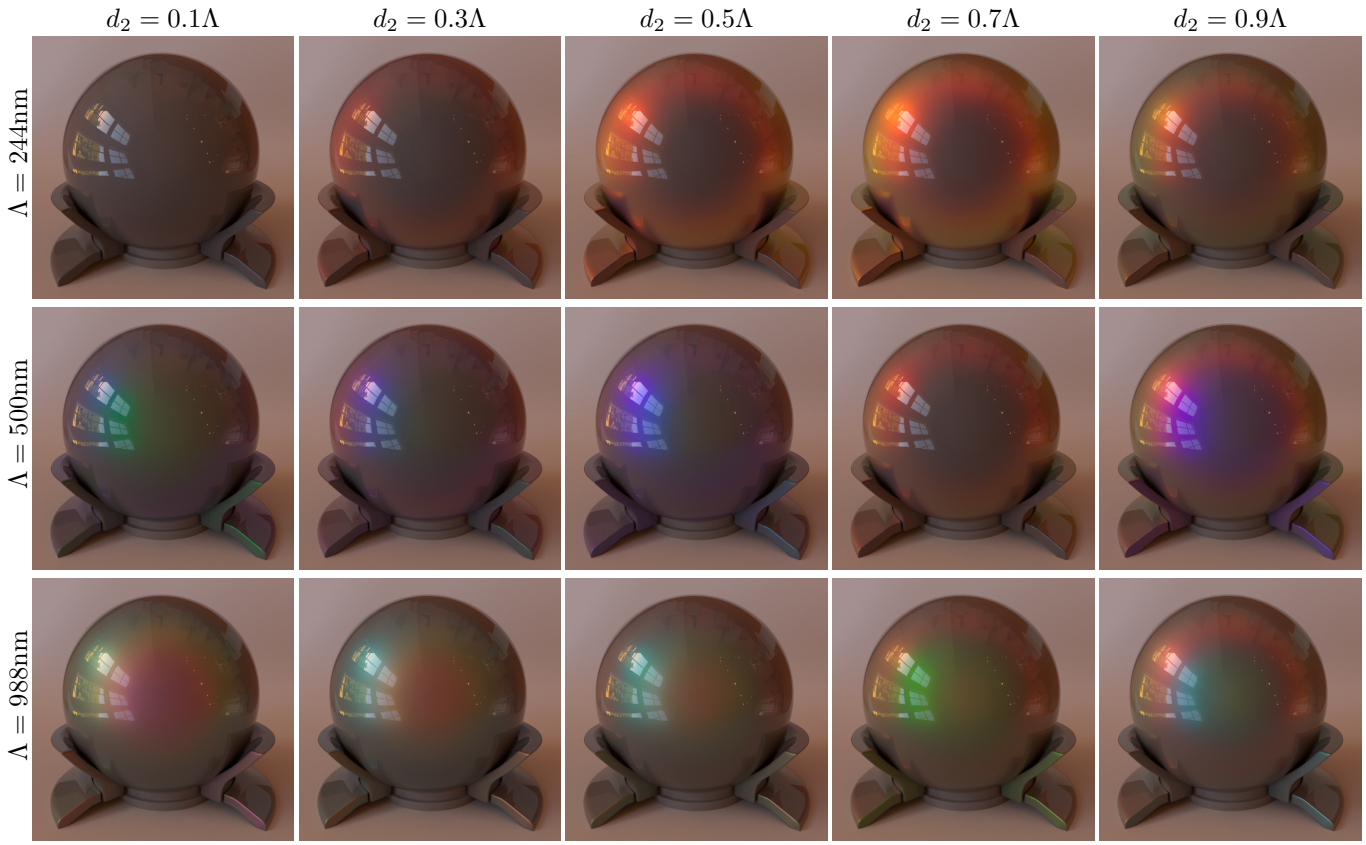

FIGURE 11 – **Exploration of coated rough Bragg appearance**, using Bragg parameters from Figure 4 in the paper, with different indices $n_1 = 1.4$ and $n_2 = 1.6$.

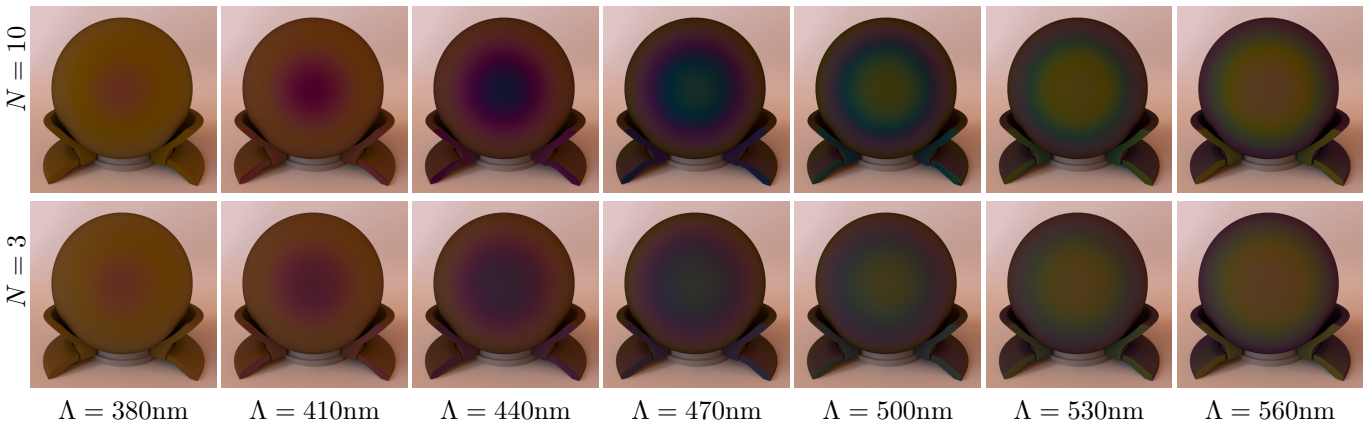

FIGURE 12 – Rendering only the diffuse component of Figure 9 (top) in the paper reveals the color variations due to transmission through the Bragg layer.